Differential double-excitation cross sections in 50–150-keV proton-helium collisions

M. Schulz, W. T. Htwe,* A. D. Gaus, J. L. Peacher, and T. Vajnai†
Department of Physics and the Laboratory for Atomic, Molecular, and Optical Research, University of Missouri–Rolla, Rolla, Missouri 65401
(Received 3 November 1994)

We have measured projectile-energy-loss spectra for 50-, 100-, and 150-keV p+He collisions. From the data we obtained differential double-excitation cross sections as a function of projectile scattering angle. At 150 keV a pronounced peak structure was observed at about 0.7 mrad for double excitation to the $(2p^2)\,^1D$ and $(2s2p)\,^1P$ states. Our data provide indications for the dominance of a first-order mechanism involving the electron-electron interaction in double excitation for 150 keV at small scattering angles. At lower projectile energies and larger scattering angles a second-order mechanism appears to be of the same order of magnitude as the first-order mechanism. In these regimes, interference effects between the first- and second-order mechanisms could be important.

PACS number(s): 34.50.Fa, 34.50.Bw

I. INTRODUCTION

One important goal of studying ion-atom collisions is to improve our understanding of the dynamics of the forces leading to an inelastic process. An inelastic atomic process can proceed through the interaction between the nucleus of one collision partner and an electron initially bound to the other collision partner (nucleus-electron interaction), or the interaction between any two electrons in the collision system (electron-electron interaction). Processes involving only one active electron (one-electron processes), such as single excitation, are usually dominated by the nucleus-electron interaction. These one-electron processes have been studied extensively for several decades both experimentally and theoretically [1–3]. As a result our understanding of the nucleus-electron interaction has improved steadily over the years, although there are still some questions which need to be addressed (e.g., the magnetic substate population in excitation processes).

In processes involving two active electrons (two-electron processes), such as double excitation, the electron-electron interaction can be quite significant, and in some cases it even dominates the nucleus-electron interaction [4,5]. Even though the underlying fundamental force is the same in both cases, there is an important difference in the dynamics between the nucleus-electron and electron-electron interactions in ion-atom collisions: in the nucleus-electron interaction a well-localized particle interacts with a diffuse electron cloud, whereas in the electron-electron interaction two diffuse electron clouds interact with each other. Such an interaction between poorly localized particles is much more challenging to treat theoretically, and thus our understanding of the electron-electron interaction is less complete than it is for the nucleus-electron interaction. As a result processes involving the electron-electron interaction have gained a lot of interest in recent years [6].

One process in which the electron-electron interaction is believed to be important is double excitation. Double excitation can proceed through a first-order or a second-order (in the projectile interaction) mechanism. In the second-order mechanism the electrons are excited through two independent interactions between the projectile nucleus and the respective electrons. The second-order process does not involve the electron-electron interaction. In the first-order mechanism the projectile nucleus interacts with only one electron. The second electron is excited by an interaction with the first electron. Another first-order double-excitation mechanism is known as shake-up [6]. In this process the projectile also interacts with only one electron. The excitation of the second electron is due to a rapid change of the effective nuclear charge of the target atom. As the first electron is excited, the screening of the nuclear charge for the second electron is reduced. As a result the second electron is not in a pure eigenstate of the new target potential. Rather, the old eigenstate is a mixture of the new eigenstates and the electron thus has some probability to be in an excited state of the new potential. Since screening itself is an effect of the electron-electron interaction, shake-up is very similar to the first-order mechanism described above in that both involve one nucleus-electron interaction and the electron-electron interaction.

The first- and second-order double excitation mechanisms lead to the same final state of the collision system and are thus indistinguishable. Therefore, the transition amplitudes for both processes have to be added coherently, which could give rise to observable interference effects in the double-excitation cross sections. Such interference effects may be observable by investigating the projectile charge dependence of the cross sections. In perturbation theory, the transition amplitude for the first-order mechanism scales linearly with Z, whereas the transition amplitude for the second-order process scales like Z^2. In the cross section, which is given by the square of the coherent sum of the transition amplitudes, this leads to a Z^3 term resulting from the cross term between both transition amplitudes. Similar arguments were used to explain differences between double-ionization cross sections

 ©1995 The American Physical Society

for protons and antiprotons colliding with helium [7,8]. There the Z^3 cross term has been interpreted as an interference between the first- and second-order double-ionization transition amplitudes. Another interpretation associates the Z^3 term to screening effects [9].

The projectile charge dependence of double-excitation cross sections has been studied by Giese *et al.* [10] for bare ions colliding with helium using Auger spectroscopy. In that work it was found that the Z dependence was significantly weaker than the Z^4 dependence expected for the pure second-order double-excitation mechanism. This was taken as an indication that the electron-electron interaction is indeed important in double excitation. However, it was not possible to determine whether there was any significant contribution from a Z^3 cross term to the cross sections. Furthermore, the analysis was complicated by another interference that can occur in double excitation, which is known as Fano interference [11]. In helium, most of the doubly excited states decay almost exclusively through autoionization. These autoionized electrons are indistinguishable from directly ionized electrons of the same energy. This leads to an interference in the electron spectra, strongly affecting the profile of the Auger lines. Because of the Fano interference it is, strictly speaking, not possible to extract double-excitation cross sections from the electron spectra.

The phase difference between the transition amplitudes for first- and second-order mechanisms, which determines possible interference patterns, depends sensitively on various collision parameters. One such parameter is the scattering angle. A total cross-section measurement integrates over all scattering angles, thereby averaging over all phase differences. This could lead to a partial or complete cancellation of possible interference effects. Any interference pattern should thus be more pronounced in the projectile angular differential cross sections, where the scattering angle, and therefore the phase difference, is determined. If interference effects could be identified, they would provide a very sensitive test of theoretical calculations which, in turn, are critical to study the dynamics of the electron-electron interaction.

Studies of double excitation are particularly interesting for protons colliding with helium, i.e., for pure two-electron collision systems. Several experimental studies have been performed on double excitation in proton-helium collisions employing Auger spectroscopy [10,12,13]. However, none of these measurements were differential in the projectile scattering angle. Recently, we have reported measured double-excitation cross sections differential in the projectile scattering angle [14]. That experiment was performed for 150-keV $p+$He collisions. Double excitation was identified in the projectile's energy-loss spectrum because it corresponds to a well-defined energy loss. In this paper we present a systematic study of double excitation in $p+$He collisions for projectile energies ranging from 50 to 150 keV.

There have been some theoretical studies of double excitation in $p+$He collisions [15–17]. The idea of an interference between first- and second-order mechanisms was used by McGuire for double ionization [8,18]. Since then it has been applied by other authors to double excitation [15,16]. Moribayashi *et al.* [15] calculated projectile angular differential double-excitation cross sections for proton and antiproton impact in the MeV/amu energy regime. They found that the first-order mechanism dominates in the excitation of the $(2s2p)\,^1P$ state, while the second-order mechanism significantly contributes to excitation of the $(2s^2)\,^1S$ and $(2p^2)\,^1D$ states. Furthermore, they found smaller differences between proton and antiproton impact than what was observed for double ionization [7], which would indicate that the Z^3 cross term in double excitation is less important than in double ionization. Recently, Morishita *et al.* [16] included direct ionization in their calculation. They found a striking difference between proton and antiproton impact in the projectile angular distribution of the cross sections. To the best of our knowledge no calculations are currently available for projectile energies as low as studied in this work (50–150 keV). However, the projectile energy dependence of the double-excitation cross sections in the work of Moribayashi *et al.* [15] and McGuire and Straton [19] indicate that the cross term is much more important at these lower energies than in the MeV/amu energy regime. The collision energies studied in the present work are not well suited for perturbation theory, and thus the Z scalings discussed for the various double-excitation terms may not hold here. Because of the potentially more significant role of the cross term, collision energies around 100 keV/amu may nevertheless turn out to be the more interesting energy regime.

II. EXPERIMENT

The experiment was performed at the University of Missouri-Rolla Ion Energy-Loss Spectrometer (UMRIELS). The experimental setup is schematically shown in Fig. 1. The details of ion energy-loss spectroscopy were described by Park [20]. In brief, a proton beam with a very narrow energy spread ($\ll 1$ eV) was produced in a hot cathode ion source and extracted at a potential of 2 kV. The ions were accelerated to energies of 50, 100, and 150 keV. After focusing, the beam was

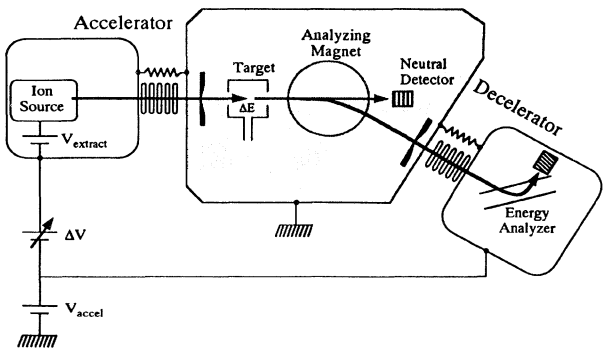

FIG. 1. Schematic overview of the University of Missouri-Rolla Ion Energy-Loss Spectrometer (UMRIELS). The neutral detector was not used in this experiment. The scattering angle is set by pivoting the accelerator around the center of the target chamber.

steered through a target gas cell containing He gas. The size of the beam was reduced to about 0.1×0.1 mm^2 by a collimator located right before the target chamber. A switching magnet was used to clean the beam from charge-changed components. After passing through a second collimator, which was used to define the projectile solid angle, the beam was decelerated by nearly the same potential as on the accelerator. Therefore, after deceleration the ions had the same energy (2 keV) as after extraction from the source. The ions were then energy analyzed by a parallel plate analyzer [21].

The analyzer was set to a fixed pass energy of 2 keV. The energy loss was scanned by applying a variable offset voltage on the accelerator relative to the decelerator. Therefore, the energy of the ions just before the collision was $E_p = e(V_{ex} + V_{dec} + V_{off})$, where V_{ex} is the source extraction voltage, V_{dec} is the decelerator voltage, and V_{off} is the offset voltage on the accelerator relative to the decelerator. If the protons suffered an energy loss of ΔE in the collision, then their energy after deceleration is $E_f = e(V_{ex} + V_{off}) - \Delta E$. Only if ΔE was equal to eV_{off}, the protons entered the analyzer with the pass energy of 2 keV and were detected. The energy loss was scanned in the regions from 19 to 25 eV and from 45 to 70 eV. The overall energy resolution was about 1.5-eV full width at half maximum (FWHM), which corresponds to a resolution relative to the collision energy of about 10^{-5}.

The scattering angle was set by pivoting the entire apparatus from the accelerator to the target chamber around the center of the target chamber. The angular resolution was determined by measuring the angular distribution of the incident beam (zero energy loss) with the target gas taken out, and was found to be about 0.15-mrad FWHM. The angular scans of the incident beams were also used to deconvolute the beam divergence from the angular distribution of the inelastically scattered projectiles [22]. The experiment was done for an angular range of 0–1 mrad.

A target gas pressure dependence was taken for projectiles which suffered an energy loss corresponding to single K to L excitation (21 eV). A linear dependence was found ensuring single-collision conditions for single excitation as well as for double excitation, since the double-excitation cross sections are much smaller than the single-excitation cross sections. The target pressure was 50 mTorr for projectile energies of 50 and 100 keV, and 70 mTorr for 150 keV. The length of the gas cell was 1 cm.

For each collision energy two measurements were performed. In the first measurement energy-loss spectra

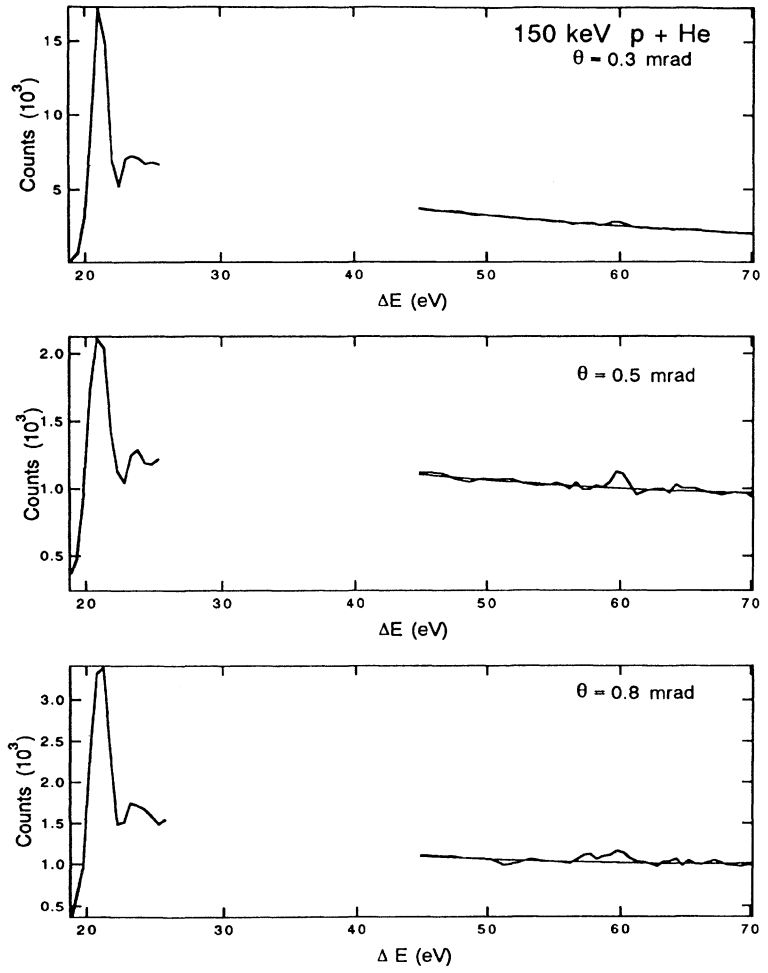

FIG. 2. Ion energy-loss spectra for 150-keV p+He collisions at three different scattering angles.

were taken at fixed scattering angles. These scans were then repeated for the scattering angles of interest. From these energy-loss spectra the ratio of the differential cross sections between double and single excitations were obtained. In the second measurement the angular distribution was measured for protons with a fixed energy loss of 21 eV corresponding to single K to L excitation. The energy resolution was found to vary somewhat for different beam tunings. However, for a given tuning the resolution did not change as a function of scattering angle. This is an expected behavior since the energy transfer to the recoil atom is only of the order of 10 meV. Therefore, the angular distribution of the count rate at the peak position of the single-excitation line is directly proportional to the differential single-excitation cross section. The cross sections were put on an absolute scale by normalizing the integrated single-excitation cross sections to known total single-excitation cross sections [23]. Therefore, these two measurements at each collision energy allowed us to determine absolute double-excitation cross sections.

III. RESULTS

In Fig. 2, energy-loss spectra are shown for 150-keV p+He collisions at scattering angles of 0.3 (top), 0.5 (center), and 0.8 mrad (bottom). Pronounced structures can be seen in these spectra. The peaks at 21 eV are due to single K to L excitation. The peaks at about 24 eV are due to excitation to the unresolved states with $n>2$. No data were taken between 25 and 45 eV. The region between 45 and 70 eV is dominated by the continuous single-ionization spectrum. Double ionization does not contribute to the energy-loss spectra in this region because the threshold for double ionization is 79 eV. The full lines show a polynomial fit to the ionization background. Double excitation to states with two L-shell electrons leads to energy losses of about 60 eV. Indeed, peak structures are observed in the energy-loss spectra of Fig. 2 around 60 eV. For a scattering angle of 0.3 mrad this peak is rather small compared to the ionization background. However, at larger scattering angles the magnitude of this peak relative to single ionization is significantly increased. At 0.8 mrad, two peaks are observed. The first peak at about 58 eV is due to excitation to the $(2s^2)\,{}^1S$ state, and the second peak contains the unresolved $(2s2p)\,{}^1P$ and $(2p^2)\,{}^1D$ states.

In our energy-loss spectra we do not observe any Fano line shapes in the double-excitation lines. This could simply be due to insufficient energy resolution. Whether the Fano line shapes observed in electron spectra should be present in the energy-loss spectra with sufficient resolution as well is still an open question. It is possible that the integration over the electron ejection angle averages out the Fano interference. Since we could not identify any Fano line shape with our energy resolution, we treat double excitation followed by autoionization and direct single ionization as if they are incoherent processes. However, we will briefly address this question again in Sec. IV.

The contribution of double excitation to the ${}^1S$ state relative to excitation to the ${}^1P$ and ${}^1D$ states depends sensitively on the projectile energy. This is illustrated for a scattering angle of 0.5 mrad in Fig. 3, which shows energy-loss spectra for this angle at projectile energies of 50 (bottom), 100 (center), and 150 keV (top). At 150 keV the ${}^1S$ state is virtually nonexistent. At 100 keV the ${}^1S$ state is observed with about half the intensity of the combined ${}^1P$ and ${}^1D$ states, and at 50 keV the corresponding peaks have about equal intensity. The importance of the ${}^1S$ state relative to the ${}^1P$ and ${}^1D$ states thus appears to increase systematically with decreasing projectile energy. This observation is consistent with the results reported by Bordenave-Montesquieu *et al.* [12]

It should be noted that with the energy-loss technique single excitation and double excitation as well as single ionization are measured simultaneously using the same detector. This means that the ratio of the double to single K to L excitation cross sections R_{DE} can be determined essentially free of systematic errors. Normalization and correction factors, such as the incident-beam intensity, the target thickness, and the detector efficiency, cancel in this ratio, which is thus given simply by the ratio of the integrated number of counts in the double-excitation peaks to the single-excitation peak. Therefore, uncertainties in these parameters do not contribute to the systematic errors.

The total number of counts in the double-excitation peaks was obtained by subtracting the polynomial fits to

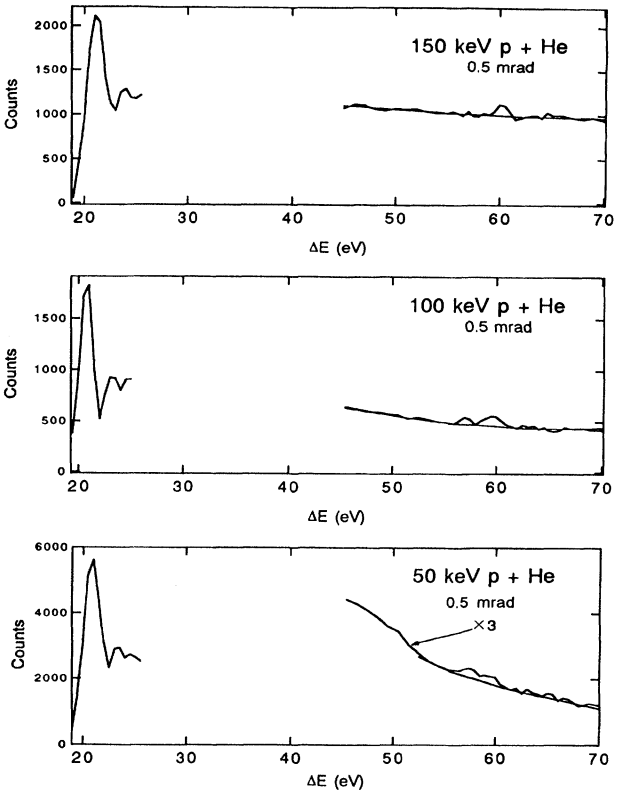

FIG. 3. Ion energy-loss spectra for a fixed scattering angle (0.5 mrad) for 50-, 100-, and 150-keV p+He collisions.

the ionization background shown in Figs. 2 and 3 from the energy-loss spectra and integrating the remaining peaks. The single-excitation peaks were fitted with Gaussian functions. The errors in R_{DE} are only given by the uncertainties in these fits and by statistical errors. These ratios are shown for the sum of the ^1P and ^1D states as a function of scattering angle in Fig. 4, and for the ^1S state in Fig. 5. At 150 keV a discernable ^1S peak was only observed for scattering angles larger than 0.7 mrad, and no reliable ratios or cross sections could be obtained for this state.

The angular dependence of R_{DE} reflects the general trend that can be seen from a qualitative inspection of the energy-loss spectra: with increasing scattering angle double excitation becomes increasingly more important relative to single excitation for all projectile energies and for both double-excitation lines resolved in the spectra. However, at 150 keV there is, apart from this general trend, a pronounced and narrow peak at about 0.7 mrad for the ^1P and ^1D states. At 50 and 100 keV, in contrast, the ratios appear to be leveling off at large scattering angles. There may be a weak structure at about 0.6 mrad for the ^1S state at 100 keV; however, this structure is smaller than the experimental uncertainties and thus is not statistically significant.

Single K to L excitation cross sections were obtained from the angular scan of the protons which lost an energy of 21 eV after deconvoluting the incident beam from the measured angular distribution, as described above [22]. The absolute magnitude was obtained by normalizing the integrated cross sections to measured total single-excitation cross sections [23]. Our differential single-excitation cross sections are shown in Fig. 6. For 50 and 100 keV our data are consistent with the cross sections measured by Park *et al.* [22] and Kvale *et al.* [24].

Absolute differential double-excitation cross sections were obtained by multiplying the single-excitation cross sections of Fig. 6 by the ratios R_{DE} of Figs. 4 and 5. Deconvoluting both the angular scans for double excitation and single excitation did not have any effect on the ratio R_{DE} compared to the values obtained without deconvolution. The differential double-excitation cross sections are shown in Figs. 7–9 for the sum of the ^1P and ^1D states for all projectile energies, and in Figs. 10 and 11 for the ^1S state for 50 and 100 keV as a function of

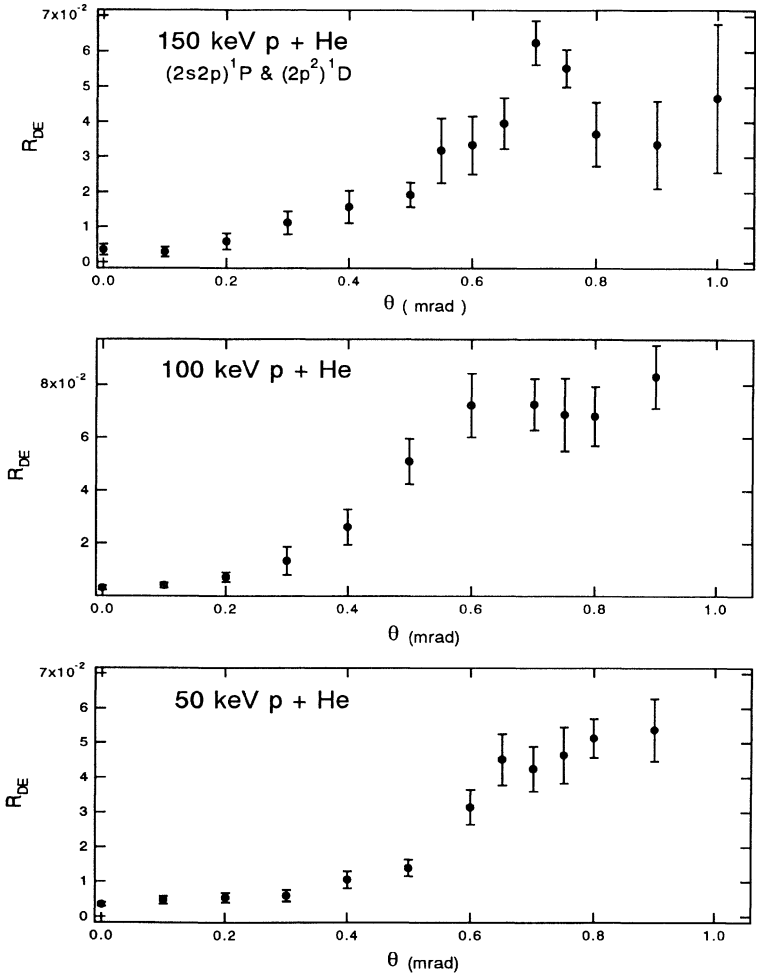

FIG. 4. Ratio of the differential double-excitation cross sections for the sum of the $(2s2p)\,^1P$ and $(2p^2)\,^1D$ states to the differential K to L single-excitation cross sections as a function of scattering angle.

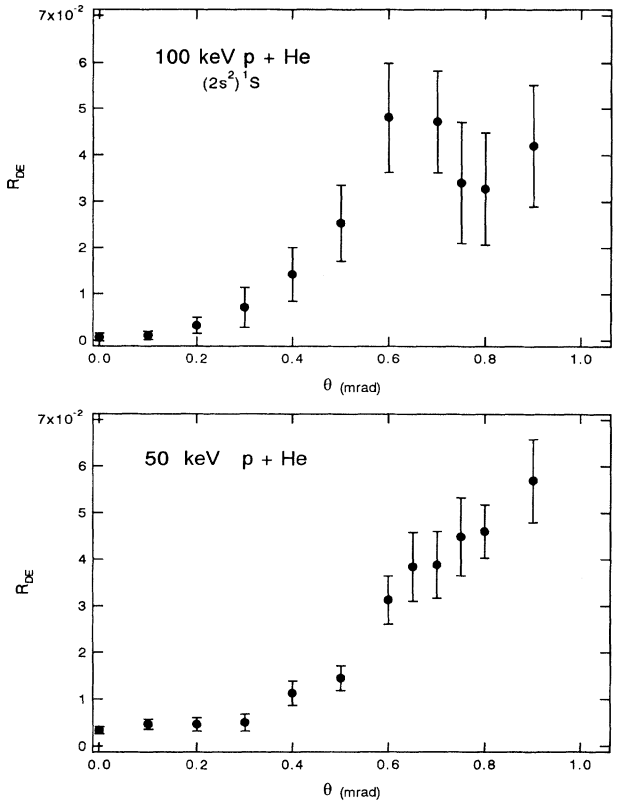

FIG. 5. Same as Fig. 1 for double excitation to the $(2s^2)\,^1S$ state.

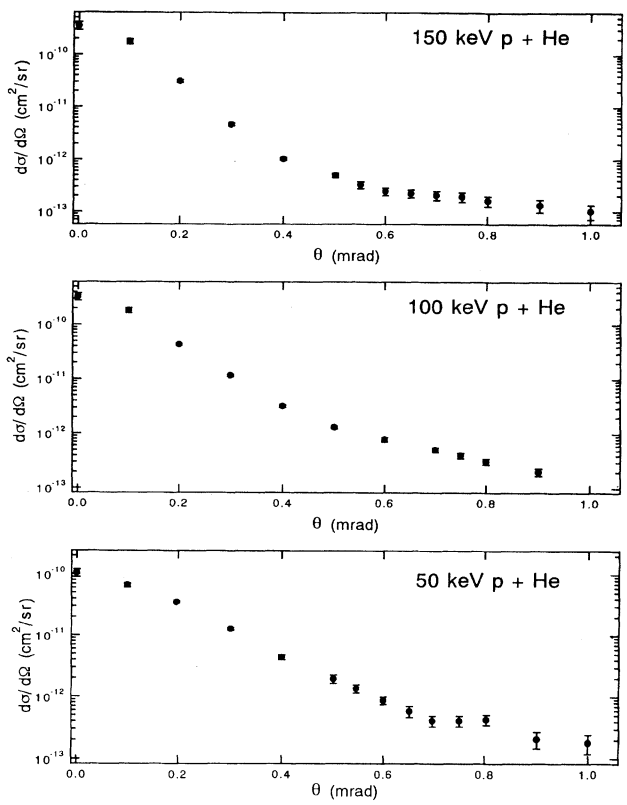

FIG. 6. Differential K to L single-excitation cross sections as a function of scattering angle.

scattering angle (closed circles). In the cross section for the sum of the ^1P and ^1D states at 150 keV, the peak observed in R_{DE} is reflected in a similar peak at 0.7 mrad. For all other cases, the cross sections just decrease rapidly with increasing angle. As mentioned above, the apparent bumps in the cross sections for 100 keV are not statistically significant. Because of the larger experimental uncertainties in the cross sections for the ^1S state, we will focus our analysis on the ^1P and ^1D states.

IV. DISCUSSION

Peak structures similar to those in R_{DE} have been observed in the corresponding ratios for double to single ionization R_{DI} [25] and for transfer ionization to single capture R_{TI} for p+He collisions [26,27]. In both cases the peak structures became less pronounced with decreasing projectile energy and were not observed in R_{TI} for projectile energies of 100 keV and below. This dependence of the peak structure on the projectile energy is consistent with our data for double excitation.

Various interpretations of the peak structures in R_{DI} and R_{TI} were reported [28–34]. Several authors used an independent-electron model to explain these structures [28–31,34]. In these calculations it is assumed that double ionization or transfer ionization proceed through two binary collisions of the proton with the two He electrons. In this binary collision model the electrons are approximated as free, so that the projectile is mainly deflected by the electrons. With these calculations the peak structures could be reproduced qualitatively; however, there are some discrepancies in the absolute magnitude. In the case of single ionization there is also strong experimental support for the importance of the projectile-target electron scattering [35,36].

In an earlier paper [14], we pointed out that in our data for double excitation the binary collision model leads to difficulties in interpreting the peak structure in R_{DE}. While the position of the peak was not inconsistent with the binary collision model, its width appeared to be narrower than what one would expect from this model. Here we point out another, more fundamental, problem. In the case of double ionization the assumption of the electrons being free is correct for the final state. Furthermore, neglecting the binding energy in the initial state is a justifiable approximation if the energy transfer to the electrons is large compared to their binding energy in the target atom. In order to have a large transfer of energy to the electrons the projectile must get relatively close to the electrons, whereas the distance of closest approach to the target nucleus is on average relatively large. Furthermore, the ionized electrons move nearly independently of the target nucleus. Therefore, it is reasonable to assume that the collision kinematics in double ionization is determined more by the electrons than by the target nucleus. In double excitation the situation is very different. Here

the energy transfer to the electrons is well determined and is evidently smaller than the binding energy of the electrons. Furthermore, the electrons remain bound to the target nucleus, which means that the final state of the collision involves only two independently moving particles. Thus the recoil angle of the target atom is unambiguously determined by the projectile scattering angle, and is very close to 90° for the scattering angles studied here. The binary collision model for a proton colliding with an electron, on the other hand, yields an electron recoil angle of about 60° for an energy transfer of 60 eV. One could try to apply this model to excitation by assuming that the electron drags the target nucleus along as it tries to escape. Because of momentum conservation, the recoil ion would then have to move at the same angle of about 60°, which is inconsistent with the recoil angle one obtains from the projectile scattering angle.

In the following we will abandon the binary collision model altogether. Rather, we will focus the discussion on the relative importance of first- and second-order double-excitation mechanisms described above. We present a simple model which qualitatively describes our experimental results. Because of the approximations being used, one should be cautious in drawing quantitative

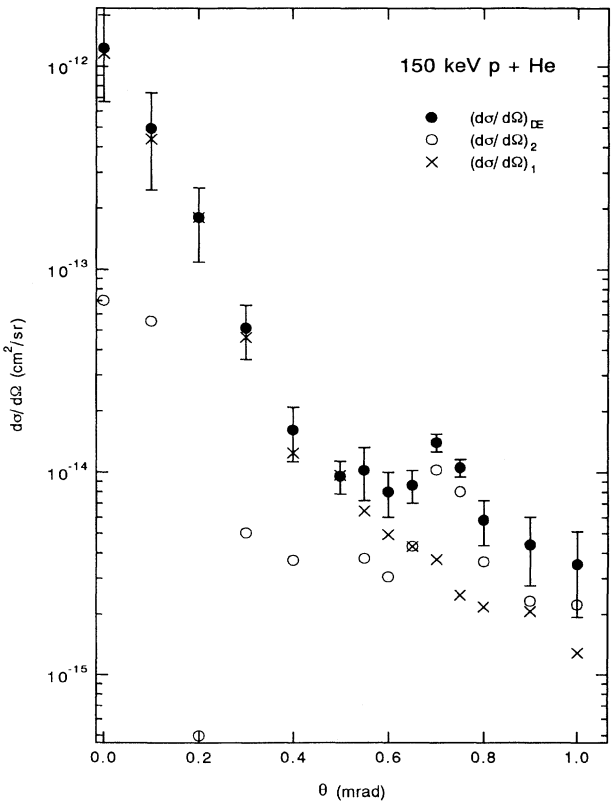

FIG. 7. Differential double-excitation cross sections for the sum of the $(2p2p)\,^1P$ and $(2p^2)\,^1D$ states (closed symbols) as a function of scattering angle for 150-keV p+He collisions. The open symbols represent the contribution from the second-order process to double excitation, and the crosses the contributions from the first-order process (see text).

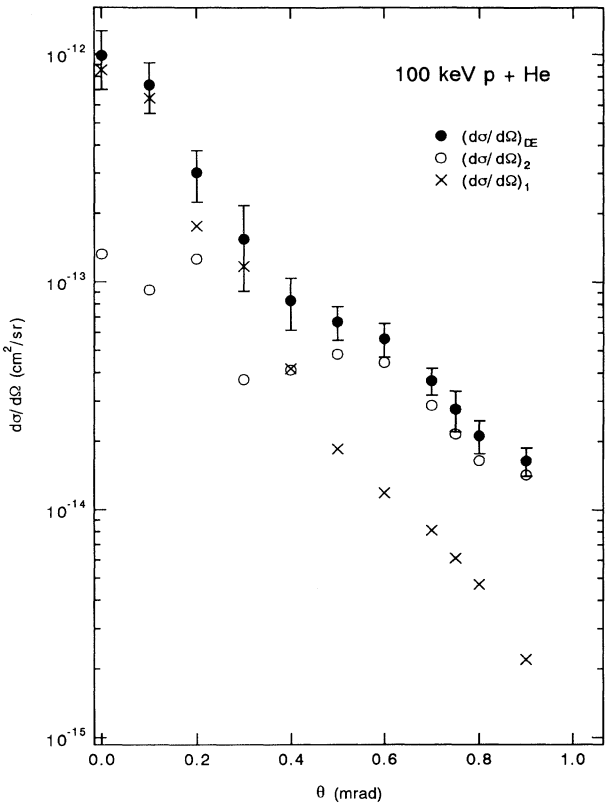

FIG. 8. Same as Fig. 7 for 100-keV p+He collisions.

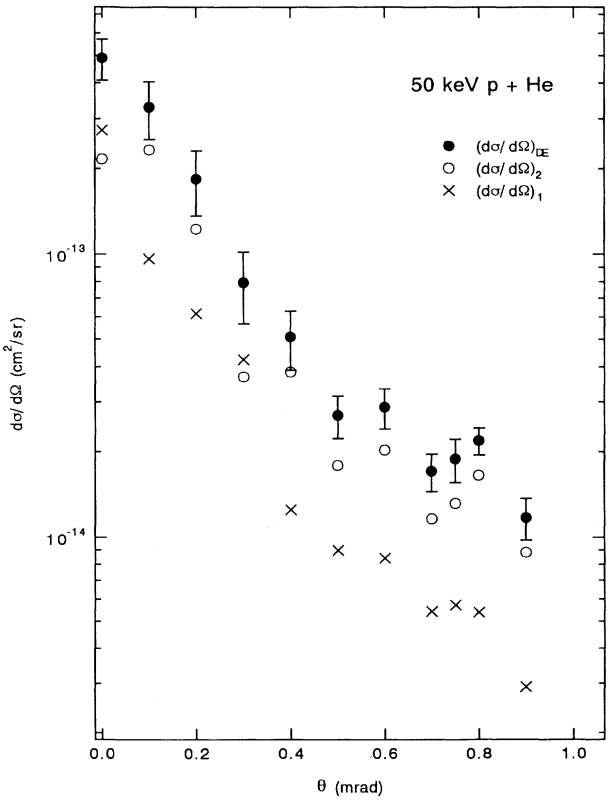

FIG. 9. Same as Fig. 7 for 50-keV p+He collisions.

conclusions. For this discussion it is useful to view the first-order mechanism as a single-ionization process followed by a time-reversed Auger decay. This is illustrated in Fig. 12. Part (a) of this figure shows the interaction of the proton with one electron. In this interaction the entire energy required for double excitation (60 eV) needs to be transferred to the electron if the proton is to interact only once. This energy transfer is sufficient to promote the electron to the continuum so that the electron is ionized. In the second part of the first-order double-excitation mechanism, which is shown in Fig. 12(b), the continuum electron interacts with the second electron, transferring part of its energy to it. As a result, the continuum electron drops to the L shell and the second electron is promoted to the L shell of the He atom. This process is just a special case of dielectronic recombination, which can be viewed as a time-reversed Auger decay.

This second part of the first-order mechanism does not involve the projectile and should thus be nearly independent of any projectile parameter such as the charge state, the projectile energy, or the scattering angle [6]. Therefore, for the first-order double-excitation mechanism we expect the same angular scattering dependence as for single ionization, leading to an energy loss of 60 eV. In the case of double ionization, the independence of the corresponding first-order mechanism of the projectile should also lead to a constant ratio R_{DI} for large projectile energies. Such a behavior has indeed been observed [25,37,38]. It should be noted that this independence of the projectile should be better fulfilled in the case of double excitation than for double ionization. For double ionization some dependence on the projectile could occur because the average energy transfer in the first interaction (between the projectile and one target electron) depends on the projectile parameters. In the case of double exci-

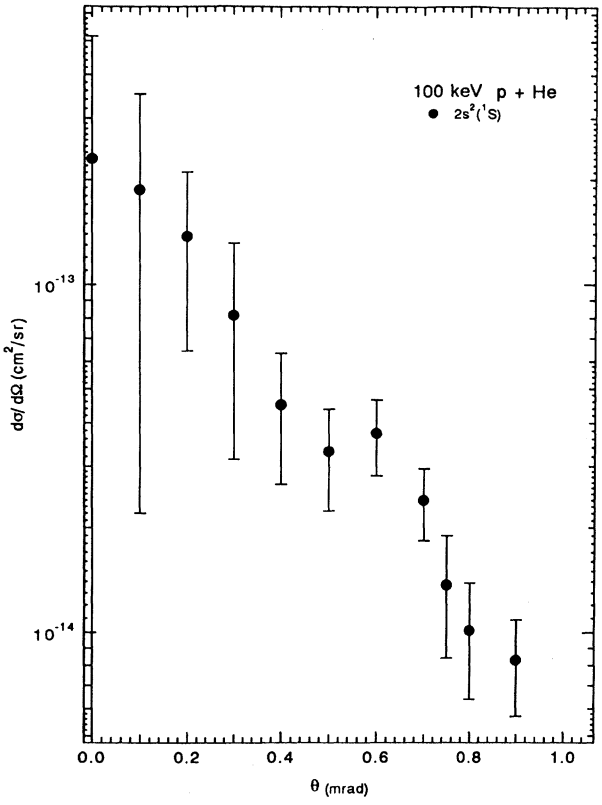

FIG. 10. Differential double-excitation cross sections for the $(2s^2)\,{}^1S$ state as a function of scattering angle for 100-keV $p+$He collisions.

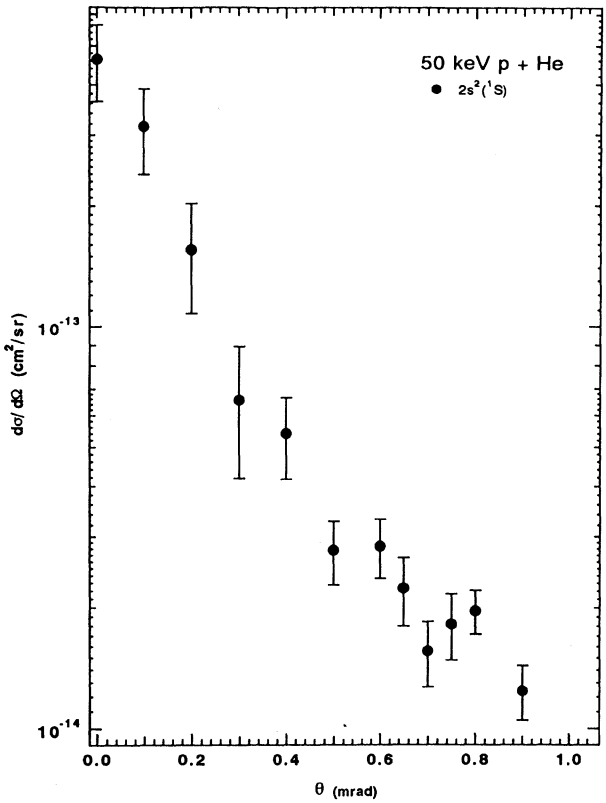

FIG. 11. Same as Fig. 10, for 50-keV $p+$He collisions.

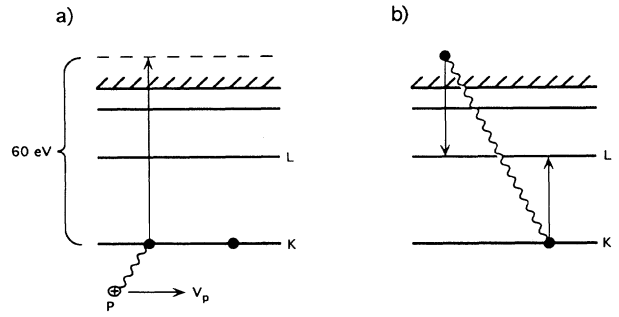

FIG. 12. Schematics of the first-order double-excitation mechanism. Part (a) shows the interaction of the projectile with one target electron. Since 60 eV of energy is transferred to the electron, this interaction leads to ionization of the electron. Part (b) shows the interaction of the ionized electron with the second target electron, which takes both electrons to the L shell of the target atom. This process can be viewed as a time-reversed Auger decay.

tation the energy transfer is well determined (60 eV).

The first-order double-excitation mechanism is expected to have a relatively weak projectile energy dependence, whereas the second-order mechanism is believed to drop relatively quickly with projectile energy [19]. Thus we expect the relative importance of the first-order mechanism to increase with increasing projectile energy. We therefore start our discussion of this point by analyzing the data for the largest projectile energy studied here (150 keV). The crosses in Fig. 7 for 150 keV show the doubly differential single-ionization cross sections for an energy loss of 60 eV, which were obtained from the polynomial fit shown in Fig. 2, multiplied by a factor to nearly match the magnitude with the measured double-excitation cross section at 0°. These cross sections are in almost perfect agreement with the double-excitation cross sections up to an angle of about 0.5 mrad. Our simple model thus suggests that up to this angle double excitation is dominated by the first-order process at this projectile energy. In the following we assume that the crosses represent the contribution from the first-order mechanism to double excitation. If this assumption is correct, then the similarity between the angular dependence of the single-ionization cross section at 60 eV and the double-excitation cross section may also be taken as an indication that at small scattering angles the Fano interference does not have a significant effect on the double-excitation cross section. If the Fano interference were important, the cross section for the first-order process would not simply be a product of the single-ionization cross section and a constant probability for the time-reversed Auger decay. Rather, we would expect the angular dependence of the cross section to exhibit some structure due to the phase difference between the direct ionization amplitude and the first-order double-excitation amplitude.

To match the magnitude of the first-order cross section with the double-excitation cross section at 0° exactly would require multiplying the ionization cross sections by a factor of $f=0.128$ eV. However, the second-order process and the cross term would then only contribute to double excitation at large scattering angles and would be zero for small angles. In order to find a more realistic contribution of the second-order process, we fitted f such that the integrated second-order cross section would yield the total double-excitation cross section obtained by using the independent-electron model. Here we make the assumption that we can treat first- and second-order processes incoherently, so that the contribution from the second-order process is given by the difference between the double-excitation cross section and the first-order cross section. However, because of the apparent dominance of the first-order process, we believe that the value of f is not significantly affected by this approximation. In the independent-electron model, the total cross section is given by

$$\sigma_{\mathrm{IEM}}=\int P_{\mathrm{SE1}}(\theta)P_{\mathrm{SE2}}(\theta)\frac{d\sigma}{d\theta_R}d\theta\ . \tag{1}$$

Here, P_{SE1} is the probability for excitation from the ground state to the $(1s2p)\,^1P$ state, P_{SE2} is the probability for excitation from the $(1s2p)\,^1P$ to the doubly excited state [e.g., $(2p^2)\,^1D$], and $d\sigma/d\theta_R$ is the Rutherford cross section. P_{SE1} was obtained by dividing our single-excitation cross sections of Fig. 6 by the Rutherford cross section. P_{SE2} is not known; however, we expect it to be significantly smaller than P_{SE1} since the excitation energy for the second electron (39 eV) is almost twice the excitation energy for the first electron (21 eV). It is reasonable to assume that P_{SE2} is very similar to the probability for ionization, leading to the same energy transfer to the electron as P_{SE2}. Since we did not take any data for energy losses between 25 and 45 eV, we use the ionization probability for 45 eV to obtain an estimate of P_{SE2}. This may be a somewhat crude approximation; however, we believe that it is a much better approximation than using the square of P_{SE1} in Eq. (1).

With this procedure we find $f=0.12$ eV, which is very close to the value required to match the first-order cross section with the double-excitation cross section at 0°. The difference between the double excitation and the first-order cross sections, which for now we assume to represent the second-order contribution to double excitation (as mentioned above, it may also contain contributions from the cross term), is shown in Fig. 7 as open circles.

It should be noted that f represents the probability for the second part of the correlated double-excitation mechanism shown in Fig. 12(b) and should thus be independent of the scattering angle and the projectile energy. Within our simple model we expect the value of f in double excitation to be significantly larger than the corresponding probability for the case of double ionization. The reason for our assumption is that the second part of the first-order process is a time-reversed Auger decay, in this case a *KLL* Auger decay. The corresponding Auger decay in double ionization is of the form $\varepsilon_1 l_1 \varepsilon_2 l_2 \rightarrow 1s\varepsilon' l'$, which has a much smaller transition rate than the *KLL* transition because of the smaller overlap of the continuum states with the ground state compared to the bound states of the L shell in the *KLL* Auger decay.

Figure 7 indicates that the contribution from the second-order mechanism to double excitation is comparable to or larger than the contribution from the first-order process only at scattering angles larger than about 0.5 mrad. It should be noted that the errors in the second-order cross section are very large, since a small fluctuation in the first-order cross section can lead to a large relative change of the second-order cross section. However, within our model, the dominance of the first-order process at small scattering angles can be stated with much less uncertainty. This means that here the cross term between both mechanisms should be negligible, since a significant cross term implies that the involved transition amplitudes are of similar magnitude. Therefore, for small scattering angles it appears to be justified to regard the open symbols as the second-order cross section. At larger angles, in contrast, the cross term could be important. Here the open symbols are thus a combination of the incoherent part of the second-order mechanism and the cross term which, of course, involves both the first- and second-order transition amplitudes. It is interesting to note that the peak structure in the double-excitation

cross sections occurs in this angular range where the cross term might be significant. It is thus quite possible that this peak is due to an interference effect.

Since f should be independent of the projectile energy, we can estimate the first-order contributions for 50 and 100 keV by using the value for f obtained from the 150-keV data and the measured ionization cross sections for an energy loss of 60 eV. The combined contributions from the second-order process and the cross term are again obtained from the difference between the double excitation and the first-order cross sections. These cross sections are shown in Figs. 8 and 9 using the same symbols as in Fig. 7. The total cross section for the second-order process plus the cross term agrees with the cross section obtained from the independent-electron model [Eq. (1)] to within 30% for 100 keV and to within a factor of 2 for 50 keV. As was seen at 150 keV the first-order contribution at 100 keV also has a very similar angular dependence to double excitation for small scattering angles. However, at 100 keV this similarity only extends to about 0.3–0.4 mrad, and the apparent dominance of the first-order process at small scattering angles does not seem to be quite as pronounced as at 150 keV. At 50 keV the contribution from both mechanisms are of the same order of magnitude over the entire angular range.

Our analysis indicates that the relative importance of the first-order mechanism may systematically increase with increasing projectile energy: at 50 keV the fraction of the correlated process in the total double-excitation cross section is about 33%, at 100 keV it is about 67%, and at 150 keV about 87% in our model. Our data also indicate that the angular range in which the cross term can be significant extends systematically to smaller scattering angles with decreasing projectile energy. Therefore, the cross term may become increasingly important with decreasing projectile energy. This could explain the increasing discrepancy between the combined total second-order and cross-term cross section, and the total cross section obtained with the independent-electron model with decreasing projectile energy.

It should be noted that the analysis described above cannot easily be applied to the ^1S state. Such an analysis requires a knowledge of the fraction of the ionization cross section leading to a continuum s electron. Because of angular momentum conservation only an s electron can lead to a $(2s^2)\,^1S$ state through a time-reversed Auger decay. Since ionization by proton impact proceeds predominantly through an electric dipole transition, one would expect ionization to produce mainly continuum p electrons.

The total double-excitation cross sections, obtained by integrating the differential cross sections, are listed in Table I. These cross sections are consistent within experimental uncertainties with the cross sections reported by Bordenave-Montesquieu *et al.* [12] using Auger spectroscopy for the same collision system.

TABLE I. Total double-excitation cross sections as a function of projectile energy for the $(2s^2)\,^1S$ state (second column), and the sum of the $(2s2p)\,^1P$ and $(2p^2)\,^1D$ states (third column).

E (keV)	^1S (cm^2)	^1P plus ^1D (cm^2)
50	$(1.1\pm0.4)\times10^{-19}$	$(1.2\pm0.4)\times10^{-19}$
100	$(9.7\pm7.0)\times10^{-20}$	$(2.1\pm0.6)\times10^{-19}$
150		$(1.2\pm0.4)\times10^{-19}$

V. CONCLUSIONS

We have systematically studied differential double-excitation cross sections as a function of projectile scattering angle for 50–150-keV p+He collisions. At 150 keV the ratio of the double- to single-excitation cross sections show a pronounced and narrow peak at about 0.7 mrad. Similar peak structures have been observed in the corresponding ratios for ionization. In the case of ionization these peak structures can be explained within a binary collision model. Here we showed that the binary collision model cannot be applied to double excitation.

The absolute differential double-excitation cross sections were analyzed in terms of the first- and second-order double excitation mechanisms. The experimental data along with our simple model indicate that the relative importance of the first-order mechanism increases with increasing projectile energy and decreasing scattering angle. At the largest projectile energy studied here (150 keV) double excitation appears to be dominated by the first-order mechanism ($\approx$90% of total double excitation). For 50 and 100 keV, in contrast, the first- and second-order mechanisms seem to be of about equal magnitude. Therefore, this intermediate projectile energy region could be a particularly interesting regime because the cross term between first- and second-order transition amplitudes might be particularly significant if the two transition amplitudes are comparable in magnitude. The peak structure observed at 150 keV at about 0.7 mrad occurs in an angular range where the contributions from the first- and second-order mechanisms are comparable, and thus it may be due to the cross term. However, definite conclusions can only be drawn after comparing our data to full theoretical calculations.

ACKNOWLEDGMENT

This work was supported by the National Science Foundation, Grant No. PHY-9020813.

*Present address: Spoon River College, Division of Arts and Sciences, R.R. 1, Canton, IL 61520.

†Present address: Department of Physics, University of Miskolc, Miskolc-Egyetemváros, H-3515, Hungary.

[1] J. T. Park, Adv. At. Mol. Phys. **19**, 67 (1983), and references therein.

[2] M. E. Rudd, Y. K. Kim, D. H. Madison, and J. W. Gallagher, Rev. Mod. Phys. **57**, 965 (1985), and references

therein.
[3] Dz. Belkic and I. Mancev, Phys. Scr. **45**, 35 (1992), and references therein.
[4] J. A. Tanis, E. M. Bernstein, W. G. Graham, M. P. Stöckli, M. Clark, R. H. McFarland, T. J. Morgan, K. H. Berkner, A. S. Schlachter, and J. W. Stearns, Phys. Rev. Lett. **53**, 2551 (1984).
[5] M. Schulz, E. Justiniano, R. Schuch, P. H. Mokler, and S. Reusch, Phys. Rev. Lett. **58**, 1734 (1987).
[6] J. H. McGuire, Adv. At. Mol. Phys. **29**, 217 (1992), and references therein.
[7] L. H. Andersen, P. Hvelplund, H. Knudsen, S. P. Møller, K. Elsener, K. G. Rensfelt, and E. Uggerhøj, Phys. Rev. Lett. **57**, 2147 (1986).
[8] J. H. McGuire, Phys. Rev. A **36**, 1114 (1987).
[9] R. E. Olson, Phys. Rev. A **36**, 1519 (1987).
[10] J. P. Giese, M. Schulz, J. K. Swenson, H. Schöne, M. Benhenni, S. L. Varghese, C. R. Vane, P. F. Dittner, S. M. Shafroth, and S. Datz, Phys. Rev. A **42**, 1231 (1990).
[11] U. Fano, Phys. Rev. **124**, 1866 (1961).
[12] A. Bordenave-Montesquieu, P. Benoit-Cattin, M. Rodiers, A. Gleizes, and H. Merchez, J. Phys. B **8**, 874 (1975).
[13] J. O. P. Pedersen and P. Hvelplund, Phys. Rev. Lett. **62**, 2373 (1989).
[14] W. Htwe, T. Vajnai, M. Barnhart, A. D. Gaus, and M. Schulz, Phys. Rev. Lett. **73**, 1348 (1994).
[15] K. Moribayashi, K. Hino, M. Matsuzawa, and M. Kimura, Phys. Rev. A **44**, 7234 (1991).
[16] T. Morishita, K. Hino, S. Watanabe, and M. Matsuzawa, in *XVIII International Conference on the Physics of Electronic and Atomic Collisions, Abstracts of Contributed Papers,* edited by T. Andersen, B. Fastrup, F. Folkmann, and H. Knudsen (IFA, Aarhus University, Aarhus, 1993), p. 527.
[17] A. Bordenave-Montesquieu, A. Gleizes, P. Moretto-Capelle, S. Andriamonje, P. Benoit-Cattin, F. Martin, and A. Salin, J. Phys. B **25**, L367 (1992).
[18] J. H. McGuire, Phys. Rev. Lett. **49**, 1153 (1982).
[19] J. H. McGuire and J. C. Straton, Phys. Rev. A **43**, 5184 (1991).
[20] J. T. Park, in *Collision Spectroscopy,* edited by R. G. Cooks (Plenum, New York, 1978), p. 19.
[21] A. D. Gaus, J. A. Brand, W. Htwe, T. J. Gay, and M. Schulz, Rev. Sci. Instrum (to be published).
[22] J. T. Park, J. M. George, J. L. Peacher, and J. E. Aldag, Phys. Rev. A **18**, 48 (1978).
[23] *Atomic Data for Fusion,* edited by C. F. Barnett (Oak Ridge National Laboratory, Oak Ridge, TN, 1990).
[24] T. J. Kvale, D. G. Seely, D. M. Blankenship, E. Redd, T. J. Gay, M. Kimura, E. Rille, J. L. Peacher, and J. T. Park, Phys. Rev. A **32**, 1369 (1985).
[25] J. P. Giese and E. Horsdal, Phys. Rev. Lett. **60**, 2018 (1988).
[26] E. Horsdal, B. Jensen, and K. O. Nielsen, Phys. Rev. Lett. **57**, 1414 (1986).
[27] S. W. Bross, S. M. Bonham, A. D. Gaus, J. L. Peacher, T. Vajnai, and M. Schulz, Phys. Rev. A **50**, 337 (1994).
[28] R. E. Olson, J. Ullrich, R. Dörner, and H. Schmidt-Böcking, Phys. Rev. A **40**, 2843 (1989).
[29] A. Salin, J. Phys. B **24**, 3211 (1991).
[30] A. Igarashi, N. Toshima, and T. Ishihara, Phys. Rev. A **45**, R6157 (1992).
[31] L. Meng, R. E. Olson, R. Dörner, J. Ullrich, and H. Schmidt-Böcking, J. Phys. B **26**, 3387 (1993).
[32] J. F. Reading, A. L. Ford, and X. Fang, Phys. Rev. Lett. **62**, 245 (1989).
[33] L. Vegh, J. Phys. B **22**, L35 (1989).
[34] R. Gayet and A. Salin, Nucl. Instrum. Methods B **56**, 82 (1991).
[35] R. Dörner, J. Ullrich, H. Schmidt-Böcking, and R. E. Olson, Phys. Rev. Lett. **63**, 147 (1989).
[36] A. Gensmantel, J. Ullrich, R. Dörner, R. E. Olson, K. Ullmann, E. Forberich, S. Lencinas, and H. Schmidt-Böcking, Phys. Rev. A **45**, 4572 (1992).
[37] E. Y. Kamber, C. L. Cocke, S. Cheng, and S. L. Varghese, Phys. Rev. Lett. **60**, 2026 (1988).
[38] H. K. Haugen, L. H. Andersen, P. Hvelplund, and H. Knudsen, Phys. Rev. A **26**, 1950 (1982).